Linear Algebra Approach to Induced Drag Minimization of an Aircraft

By Hong-su NAM,[1)] and Hak-tae LEE[1)]

[1)] *Department of Aerospace Engineering, Inha University, Incheon, Korea*

In general, induced drag of a single wing is minimized when the lift distribution is elliptic. However, most aircraft obtain longitudinal stability by using a horizontal tail. Even if the main wing has an elliptic lift distribution, the induced drag of the whole aircraft is not minimized at the trim condition. This paper presents a method to find the twist angle distribution that minimizes the induced drag of the whole aircraft using a vortex panel method combined with linear algebra techniques. With a given set of constraints such as fixed lifts at the main wing and the tail, induced drag is expressed as a quadratic form of the twist distribution. As the solution is not unique, an additional objective is proposed to find an optimal distribution. The proposed methodology is tested with three example designs and compared with AVL. Depending on the design, as much as five percent reduction in the induced drag is achieve while maintaining the given trim condition.

Key Words: Induced Drag Minimization, Trim Condition, Lifting Line Theory, Quadratic Form

Nomenclature

L	:	lift
D_{ind}	:	induced drag
ρ	:	air density
U_∞	:	freestream speed
Δy_j	:	spanwise panel width
Γ_j	:	strength of the horseshoe vortex
w_j	:	downwash at the Trefftz plane
$\mathbf{\Gamma}$	:	strength of horseshoe vortex vector
$\boldsymbol{\theta}$	:	twist angle vector
$[AIC]$	:	Aerodynamic influence coefficient
$\mathbf{w}$	:	downwash vector
C_L	:	lift coefficient
$C_{D_{ind}}$	:	indcued drag coefficient
e	:	inviscid span efficiency

1. Introduction

In general, designers use multidisciplinary optimization to design aircraft. Therefore, although the induced drag may not be at its minimum, the design that minimizes the final objective function is selected. However, the importance of the induced drag increases when a large lift coefficient is required at nominal flight condition such as in high-altitude long-endurance aircraft or in human-powered aircraft.

It is well known that the induced drag is minimized when the lift distribution becomes elliptic.[1,2)] with an assumption of incompressible inviscid flow and planar wakes. However, most aircraft requires a horizontal tail to obtain longitudinal stability. Even if the main wing with an elliptic lift distribution is used, the induced drag of the whole aircraft is not minimized at the trim condition. The additional drag caused by achieving trim with a given static margin is called trim drag.

As a related study to reduce induced drag, Phillips *et al.*[3)] calculated the twist distribution to minimize induced drag using Prandtl's classical lifting-line theory and Fourier series for a single wing. Kolonay and Eastep[4)] presented a method to reduce induced drag using a control surface on a flexible wing. Munk[5)] showed that nonplanar wings could have significantly lower induced drag compared to planar wings with the same span and lift.

This paper presents a technique to find a design that eliminates this trim drag. Although it is known that the trim drag can be made to zero,[6)] there has not been a clear presentation about how to find the actual geometry. This paper assumes that the planform and the relative positions of the main wing and the tail are fixed. With a set of given constraints such as the total lifts of the main wing and the tail, the twist angle distribution that minimizes the induced drag of the wing tail combination is calculated using linear algebra techniques. The proposed techniques are applied to three examples to show the effectiveness.

The structure of this paper is as follows. Section **2.** briefly describes the vortex panel method used in this paper. Section **3.** shows the linear algebra formulation to find the twist angle distribution. Section **4.** shows the results of applying the techniques of this paper to three different designs. Finally, Section **5.** summarizes and concludes the paper.

2. Vortex Panel Method

Vortex panel method developed from Prandtl's lifting line theory is a method that can divide the wing into multiple spanwise panels and distribute the horseshoe vortex to each panel to calculate the lift and induced drag of the three-dimensional wing, as shown in Eq. (1) and Eq. (2).[2,7)] Note that Eq. (2) is expressed in the Trefftz plane where w_j are the downwash calculated at the far field.

$$L = -\rho U_\infty \sum_{j=1}^{n} \Gamma_j \Delta y_j \tag{1}$$

$$D_{ind} = -\frac{\rho}{2} \sum_{j=1}^{n} \Gamma_j w_j \Delta y_j \tag{2}$$

The horseshoe vortex consists of a bound vortex and trailing vortices. The bound vortex is placed at the quarter chord line of each panel, and the trailing vortices are two semi-infinite lines

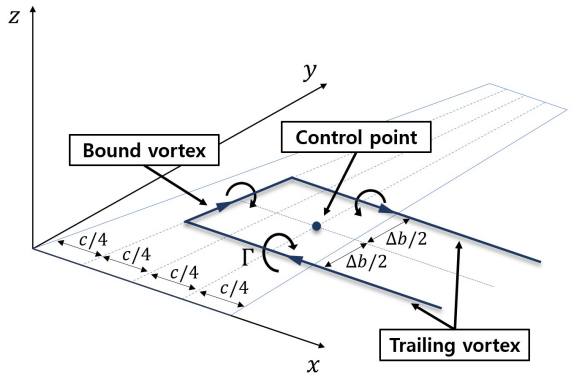

Fig. 1. The horseshoe vortex and the control point on the wing.

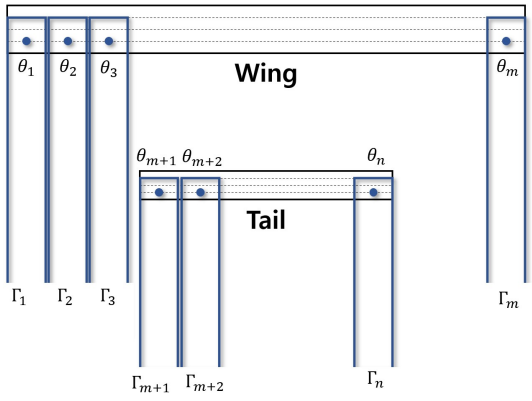

Fig. 2. The matrix indices definition.

extending back infinitely from both ends of the bound vortex in the freestream direction.[7,8)]

This paper uses Weissinger[9)]'s method that uses a single chordwise panel and positions the control points at three-quarter chord positions for the aerodynamic analysis. Bound vortices and wakes are assumed to be on the same plane for each lifting surface, and the wake deformation is not considered. Effects from angle-of-attack, twist angle, and cambers are all aggregated together as the surface normal direction at the control points. Figure 1 shows the coordinate system, one panel, horseshoe vortex, and the control point on a wing.

3. Linear Algebra Formulation

In this paper, as shown in Fig. 2, matrix indices are defined from left to right of the main wing from 1 to m and from left to right of the horizontal tail from m+1 to n. Symmetry is not considered to be able to handle non-symmetric lift distribution. The boundary condition that causes the normal velocity component of the wing surface to be zero at the control points can be expressed as in Eq. (3) assuming small angles.

$$[AIC]\boldsymbol{\Gamma} = -U_\infty \boldsymbol{\theta} \tag{3}$$

Various constraints such as total lift, surface lifts, or rolling moments can be imposed in the form of linear sum of the lifts generated from each horseshoe vortex as shown in Eq. (4). If p constraints are imposed, $\mathbf{L}$ is a p by 1 vector and $\mathbf{D}$ is a p by n matrix. Generally, p is much smaller than n .

$$\rho U_\infty \mathbf{D}\boldsymbol{\Gamma} = \mathbf{L} \tag{4}$$

By combining Eqs. (3) and (4), the relationship between $\boldsymbol{\theta}$ and $\mathbf{L}$ can be found in Eq. (5).

$$\rho {U_\infty}^2 \mathbf{D}\mathbf{A}\boldsymbol{\theta} = \mathbf{L} \tag{5}$$

where

$$\mathbf{A} = -[AIC]^{-1} \tag{6}$$

If $\boldsymbol{\theta}_0$ is an arbitrary solution that satisfies Eq. (5), $\boldsymbol{\theta}$ can be expressed as in Eq. (7) for an independent variable $\mathbf{y}$. $\mathbf{F}$ is the orthonormal basis of the null space of $\mathbf{DA}$.

$$\boldsymbol{\theta} = \mathbf{F}\mathbf{y} + \boldsymbol{\theta}_0 \tag{7}$$

Downwash at the Trefftz plane, $\mathbf{w}$, is a linear combination of Γs and can be expressed as in Eq. (8). $\mathbf{E}$ is the influence coefficient for the downwash in the Trefftz plane.

$$\mathbf{w} = \mathbf{E}\boldsymbol{\Gamma} \tag{8}$$

Since both $\boldsymbol{\Gamma}$ and $\mathbf{w}$ can be expressed as functions of $\boldsymbol{\theta}$, the induced drag becomes a quadratic form of $\boldsymbol{\theta}$, as shown in Eq. (9). $\mathbf{G}$ is a diagonal matrix with all the spanwise panel widths

$$D_{ind} = \frac{1}{2}\rho \boldsymbol{\Gamma}\mathbf{G}\mathbf{w} = \left(\frac{1}{2}\rho {U_\infty}^2\right)\boldsymbol{\theta}^{\mathrm{T}}\mathbf{A}^{\mathrm{T}}\mathbf{G}\mathbf{E}\mathbf{A}\boldsymbol{\theta} \tag{9}$$

In conclusion, as shown in Eq. (10), it becomes a problem to find $\mathbf{y}$ that minimizes the objective function J_1 that represents the induced drag.

$$J_1 = (\mathbf{F}\mathbf{y} + \boldsymbol{\theta}_0)^{\mathrm{T}}\,\mathbf{A}^{\mathrm{T}}\mathbf{X}\mathbf{A}\,(\mathbf{F}\mathbf{y} + \boldsymbol{\theta}_0) \tag{10}$$

Since induced drag is always positive, $\boldsymbol{\theta}^{\mathrm{T}}\mathbf{A}^{\mathrm{T}}\mathbf{G}\mathbf{E}\mathbf{A}\boldsymbol{\theta}$ is always positive regardless of $\boldsymbol{\theta}$. However, $\mathbf{GE}$ may not be symmetric. If $\mathbf{X}$ is defined as in Eq. (11), then the $\mathbf{y}$ that minimizes J_1 must satisfy Eq. (12).

$$\mathbf{X} = \frac{\mathbf{G}\mathbf{E} + (\mathbf{G}\mathbf{E})^{\mathrm{T}}}{2} \tag{11}$$

$$\mathbf{A}_2\mathbf{y} = \mathbf{b}_2 \tag{12}$$

where

$$\mathbf{A}_2 = \mathbf{F}^{\mathrm{T}}\mathbf{A}^{\mathrm{T}}\mathbf{X}\mathbf{A}\mathbf{F} \tag{13}$$

$$\mathbf{b}_2 = -\mathbf{F}^{\mathrm{T}}\mathbf{A}^{\mathrm{T}}\mathbf{X}\mathbf{A}\boldsymbol{\theta}_0 \tag{14}$$

However, $\mathbf{A_2}$ generally does not have a full rank, which means there are multiple twist distributions that minimizes the induced drag. To obtain a single the solution, additional condition is necessary. In this study, minimization of the objective function shown in Eq. (15) is used. Through this objective function, solutions with excessive twist angles will not be selected.

$$J_2 = \boldsymbol{\theta}^{\mathrm{T}}\boldsymbol{\theta} \tag{15}$$

Similar to Eq. (7), if $\mathbf{H}$ is the orthonormal basis of the null space of $\mathbf{A_2}$, $\mathbf{y}$ can be expressed as in Eq. (16).

$$\mathbf{y} = \mathbf{H}\mathbf{z} + \mathbf{y}_0 \tag{16}$$

$\mathbf{z}$ that minimizes Eq. (15) can is found using the expression for the minimum of a quadratic form again. The final solution, $\boldsymbol{\theta}^*$, is expressed as in Eq. (17), which is the twist distribution

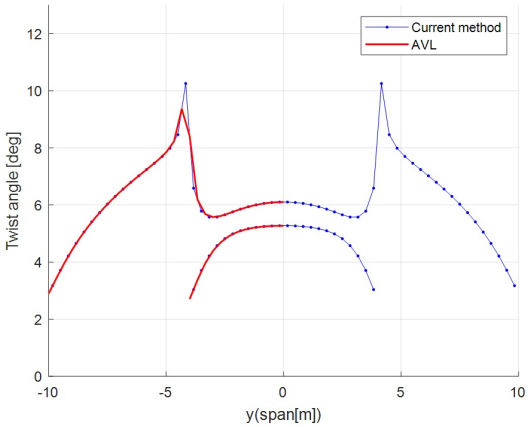

Fig. 3. Case1 twist angle distribution.

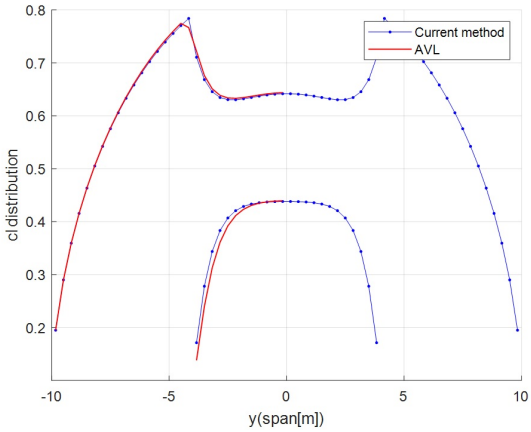

Fig. 4. Case1 lift coefficient distribution.

that minimizes the induced drag while satisfying all the constraints in Eq. (4)

$$\boldsymbol{\theta}^* = \mathbf{F}\mathbf{H}\mathbf{z}^* + \mathbf{F}\mathbf{y}_0 + \boldsymbol{\theta}_0 \tag{17}$$

where

$$\mathbf{z}^* = -(\mathbf{F}\mathbf{H})^{\mathrm{T}}(\mathbf{F}\mathbf{y}_0 + \boldsymbol{\theta}_0) \tag{18}$$

4. Example Results

Three test cases are presented in this section. In all cases, symmetric airfoil is assumed. Lifts of the main wing and the tail are used as constraints, so that the trim condition is maintained after optimizing the twist distribution. The results are compared to those calculated using AVL.[10)]

4.1. Case 1 (Test case)

Case1 analyzes the results for an aircraft with a rectangular main wing and a horizontal tail. The specifications of the aircraft are shown in Table 1.

Table 1. Case1 aircraft specifications.

	Wing	Tail
span	20 m	8 m
chord	1.0 m	0.5 m
lift coefficient	0.61	0.39
Root LE distance	5 m	

In Fig. 3, the blue line represents the twist angle distribution that minimizes the two objective functions as in Eqs. (10) and (15). Moreover, the red line is the twist angle distribution used for the input to AVL to cross-validate the results. Figure 4 shows the C_l distribution along with the AVL results that closely match the current study.

Table 2 compares the induced drag coefficient and span efficiency before and after the optimization. Lift coefficients of wing and tail as well as the sate of trim before and after the optimization, stay identical, but with the optimized twist distribution, it can be seen that the induced drag is reduced by more than five percent, and the span efficiency becomes one.

Table 2. Case1 result and comparison

	Before	After	
	AVL result	current method	AVL result
C_L	0.68	0.68	0.68
$C_{D_{ind}}$	0.00794	0.00728	0.00737
e	0.93	1.02	1.02

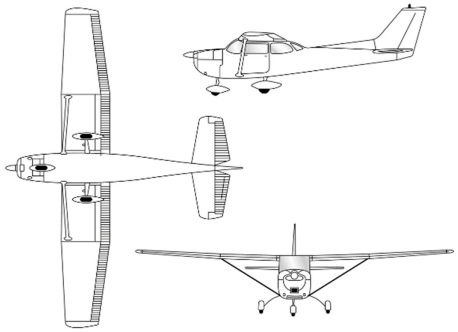

Fig. 5. Cessna172 geometry.

4.2. Case 2 (Cessna 172)

Figure 5 shows a representative general aviation aircraft, Cessna172. In Case 2, the optimization techniques are applied to the geometry of Cessna 172. Flight conditions are assumed to be 3,000 m altitude, a mass of 1,111 kg, and 122 knots cruise speed. Assuming that the static margin is 19 percent, the main wing and tail lift coefficients in trim conditions are 0.37 and -0.04, respectively.

The results are shown in table 3. In the case of Cessna 172, span efficiency in the trim condition was already one before optimization. As can be seen in Fig. 7, C_l distribution before and after the optimization does not display a noticeable difference. This result is expected in the sense that this popular aircraft already have a good aerodynamic characteristic with a tail that is lightly loaded at the trim condition.

4.3. Case 3 (Inha University Human-Powered Aircraft)

AOA15 is a human-powered aircraft[11,12)] built by the students of Inha University in 2015. The dimensions are shown in Fig. 8. The aircraft was purposely designed to have a large lifting tail to enable a smaller wingspan for easier transportation. The main wing and tail lift coefficients in the trim conditions are 1.07 and 0.56, respectively. In the case of a human-powered air-

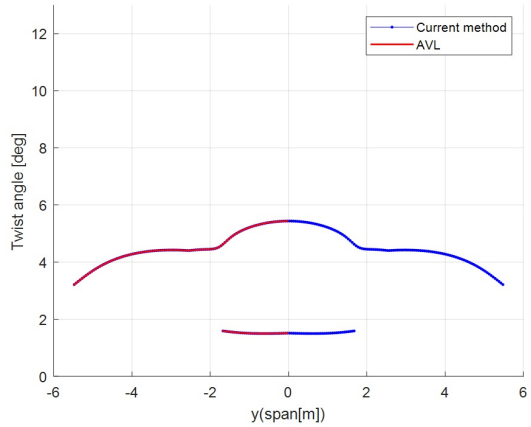

Fig. 6. Case2 twist angle distribution.

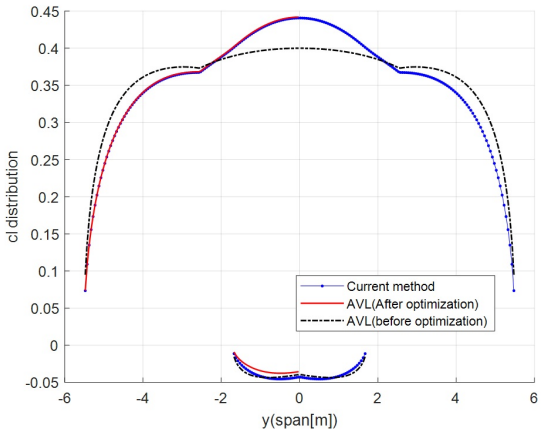

Fig. 7. Case2 lift coefficient distribution.

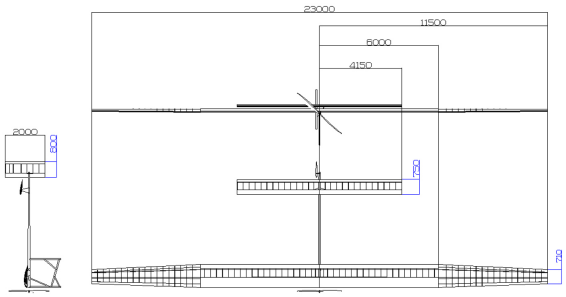

Fig. 8. AOA 15 geometry.

craft that must fly at a high C_L to minimize the required power, the induced drag is much larger than any other drag.

Optimal twist distribution assuming symmetric airfoil is shown in Fig. 9 that has up to thirteen-degree variation in the twist angle. Note that this is a solution found for a symmetric airfoil. The induced drag can be minimized with an overall lower twist angle distribution when cambered airfoils are strategically used.

As the height difference between the main wing and the tail increases, the span efficiency does not become one even after the optimization. Another variation of the AOA15 design that places the main wing and the tail on the same plane is also tested. Figs. 11 and 12 show the twist distribution and the

Table 3. Case2 result and comparison

	Before	After	
	AVL result	current method	AVL result
C_L	0.36	0.36	0.36
$C_{D_{ind}}$	0.00575	0.00572	0.00581
e	1.00	1.00	1.00

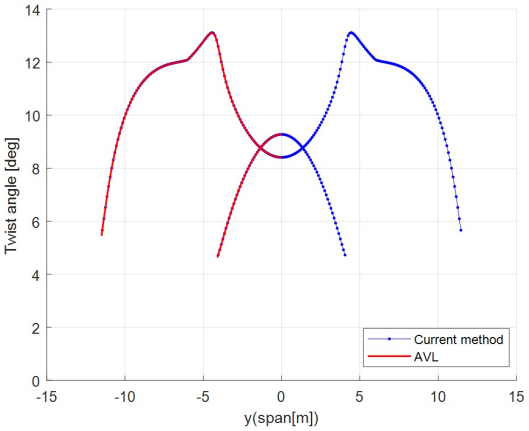

Fig. 9. Case3-1 twist angle distribution.

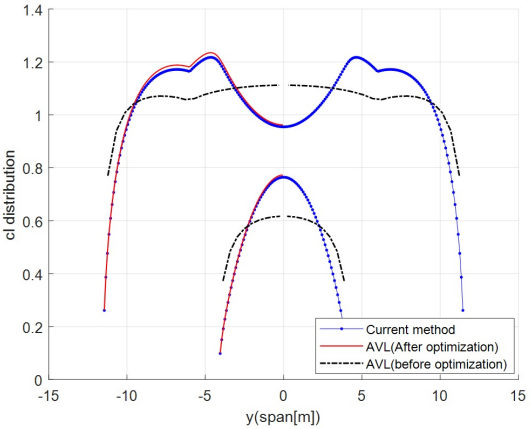

Fig. 10. Case3-1 lift coefficient distribution.

C_l distribution, respectively, for this modified design. Table 4 shows the comparison of the three AOA15 results.

If the vertical separation is maintained, the optimized twist distribution results in a 2.7 percent smaller induced drag. If the vertical separation is removed, the reduction becomes 5.4 percent, which can be significant depending on the application.

Table 4. Case3 result and comparison

	Before	After (Case3-1)		After (Case3-2)	
	AVL result	current method	AVL result	current method	AVL result
C_L	1.21	1.21	1.22	1.21	1.22
$C_{D_{ind}}$	0.0223	0.0217	0.0221	0.0211	0.0218
e	0.95	0.98	0.98	1.00	1.00

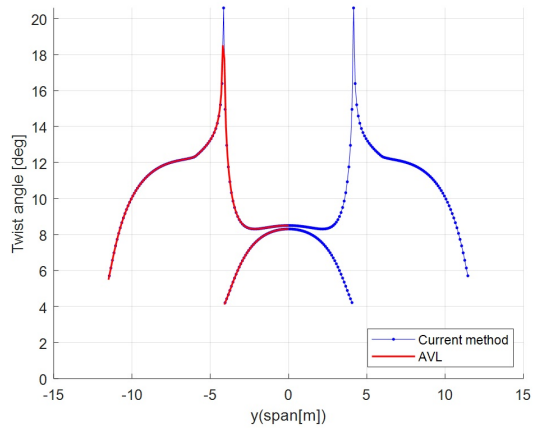

Fig. 11. Case3-2 twist angle distribution.

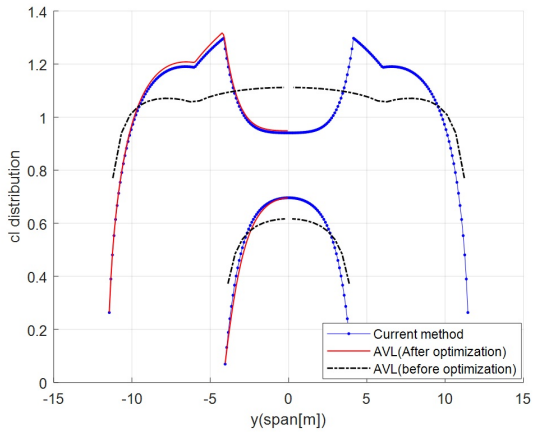

Fig. 12. Case3-2 lift coefficient distribution.

5. Conclusion

This paper presents a method to find the twist angle distribution that minimizes the induced drag of the entire aircraft using vortex panel method and linear algebra techniques. In the process, an additional objective function that minimizes the square sum of the twist angle is introduced to make the solution unique. The methods were applied to three aircraft and demonstrated that it is possible to achieve theoretically minimum induced drag while maintaining the same trim conditions. Those results are also verified against a widely used tool, AVL. The current study is theoretical and sometimes produces an unrealistic twist distribution. However, the methodology can be useful for optimizing the designs that are dominated by induced drag, especially, if the tail is large and heavily loaded.

Acknowledgments

This work is supported by Inha University and the Korea Evaluation Institute of Industrial Technology grand funded by Ministry of Trade, Industry and Energy (Grant 20016489).

References

1) ANDERSON, J.: *Fundamentals of aerodynamics (6th ed.)*, McGraw-Hill Education, New York, 2016, pp. 442–446.
2) Kroo, I.: Drag due to lift: concepts for prediction and reduction, Annual review of fluid mechanics, 2001, pp. 590–601.
3) Phillips, W. F., Fugal, S. R., Spall, R. E.: Minimizing Induced Drag with Wing Twist, Computational-Fluid-Dynamics Validation. Journal of Aircraft, **43**(2), 2006, pp. 437—444.
4) Kolonay, Ra. M., Eastep, F.: Optimal Scheduling of Control Surfaces Flexible Wings to Reduce Induced Drag. Journal of Aircraft, **43**(6), 2006, pp. 1655-–1661.
5) Munk, M.: The Minimum Induced Drag of Aerofoils, NACA Technical Rept, No. 121, 1921.
6) Larrabee, E. E.: Trim drag in the light of Munk's stagger theorem, *Kansas Univ. Proc. of the NASA, Ind., Univ., Gen. Aviation Drag Reduction Workshop*, 1975.
7) Katz, J., Plotkin, A.: *Low-speed aerodynamics (Vol. 13)*, Cambridge university press, 2001, pp. 331–338
8) Lee, C. H., Kang, H. M., Kim, C. W.: Analysis of the Influence of Ground Effect on the Aerodynamic Performance of a Wing Using Lifting-Line Method, *Journal of the Korean Society for Aeronautical and Space Sciences*, **42.4** (2014), pp. 298–304.
9) Weissinger, J.: The Lift Distribution of Swept-Back Wings, NACA TM-1120, 1947.
10) Drela, M. and Youngren, H.: AVL 3.30 UserPrimer, Department of Aeronautics and Astronautics,Massachusetts Institute of Technology, 2010, pp. 1–39.
11) Kwon, K. J., Park, B. S., Kang, S. Y., Lee, H. Y., Lee. H. T.: Techniques to Analyze Bracing Wires in Human Powered Aircraft. The Korean Society for Aeronautical and Space Sciences, 2016, pp. 678–680.
12) Kwon, K. J., Lee, H. T.: Korea Human Powered Aircraft Competition Lessons Learned, In AIAA Scitech 2020 Forum, 2020.